GEOPHYSICAL RESEARCH LETTERS, VOL. 20, NO. 17, PAGES 1843-1846, SEPTEMBER 3, 1993

LOW P-WAVE VELOCITY AT THE BASE OF THE MANTLE

Edward J. Garnero[1], Stephen P. Grand[2], and Donald V. Helmberger[1]

Abstract. A tool for investigating P-wave (V_P) structure at the base of the mantle is presented. SKS waves at distances around 107° are incident upon the core-mantle boundary (CMB) with a slowness that allows for coupling with diffracted P-waves (P_d) at the base of the mantle. The P-wave diffraction occurs at both the SKS entrance and exit locations of the outer core. The resulting phase, SP_dKS, arrives slightly later in time than SKS, having a wave path through the mantle and core very close to SKS. The difference time between SKS and SP_dKS most strongly depends on V_P at the base of the mantle near SKS core entrance and exit points. Digitized long-period (5-15s) observations from deep focus Tonga events recorded by North American WWSSN and Canadian Seismographic Network stations, and South American events recorded by European and Eurasian WWSSN stations exhibit anomalously large SP_dKS-SKS difference times. SKS and the later arriving SP_dKS are separated by several seconds more than predictions made by the global average PREM model. Models having a pronounced low-velocity zone in V_P at the base of the mantle best predict the observations. These models are perturbations of the PREM model, whereby the lowermost 50-100 km of the D″ layer has a negative V_P gradient, with the mantle-side CMB V_P reduced from PREM by 5% (to 13.0 km/s) at the base of the mantle.

Introduction

Knowledge of the core-mantle boundary (CMB) region is based entirely on data gathered near the Earth's surface. Our probes of the interior include seismic waves and free oscillations, tides, gravity, heat flow, rotation of the Earth, electric and magnetic field measurements, and information from rocks transported to the surface by dynamic geological processes. Interpreting these data often requires assuming an initial Earth model constructed using previously determined knowledge of the region. In most CMB studies, this knowledge comes from past seismic investigations. A more detailed understanding of the seismic structure of the CMB region will have a strong influence on many other geophysical disciplines.

In this paper, an important seismic constraint on the P-wave velocity (V_P) structure at the base of the mantle is presented. SKS waves near 107° in epicentral distance have an angle of incidence to the CMB that is the critical angle of incidence for ScP waves. At such a ray parameter, SKS couples with diffracted P-waves (P_d) along the mantle side of the CMB at SKS core entrance and exit locations, to make a later arriving phase named SP_dKS. This phase was theoretically discussed by Kind and Müller [1975] and Choy [1977], and shown to have a travel-time curve with the same slope as that for P_d, and tangential to the travel-time curve of SKS at around 107° (this distance is a model dependent feature). Observations of SP_dKS were noted by Schweitzer [1984] and Schweitzer and Müller [1986] in studies of SKS and SKKS, but travel time and waveshape of SP_dKS have not been explored for modeling purposes. An interrelated phenomena, however, is the drop in SKS amplitudes as seen in SKKS/SKS ratios due to losing SKS energy to the SP_dKS phase [Silver and Bina, 1993]. SP_dKS becomes visibly separate from SKS near 109°-110°, with the SP_dKS-SKS difference time increasing with distance. Figure 1a shows a ray-path representation of SKS and SP_dKS waves at 118° distance (for a 500 km deep source). The figure shows two different paths (SP_dKS + SKP_dS) contributing to the composite diffraction arrival. However, as pointed out by Choy [1977], there are an infinite number of such paths between the two end-members shown in the figure that connect the source and station (i.e., SP_dKP_dS waves). These paths travel partly as a P-wave in the core (K) and partly as P_d in the mantle, all having in common the same total angular distance traveled by P_d+K. Figure 1b presents the separation of SKS and SP_dKS wave paths as they cross the CMB. The dotted line gives the distance between the S leg of SKS and SP_dKS raypaths at the CMB, which at 125°, is only around 220 km. This suggests that S-wave velocity (V_S) structure in the mantle is not likely to strongly affect SP_dKS-SKS times or waveforms, due to the similarity of

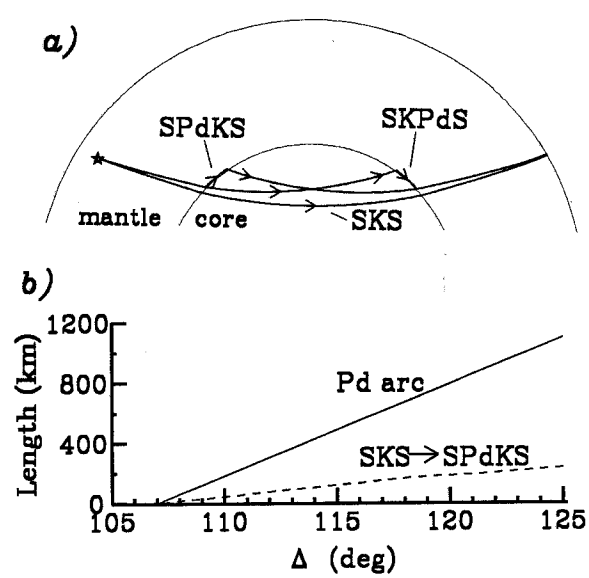

Fig. 1. (a) Cross-section showing ray paths of SKS and the two end-member SP_dKS paths (of the infinite set of rays comprising SP_dKS, see text). (b) Length of P diffraction arcs (solid line); and distance between S legs of SKS and SP_dKS at base of mantle (dashed line).

[1]Seismological Lab., California Institute of Technology
[2]Department of Geological Sciences, University of Texas

Paper number 93GL02009
0094-8534/93/93GL-02009$03.00

the mantle paths. The solid line represents the total length (source + receiver side) of the P_d arc for any of the infinite paths comprising SP_dKS.

The purpose of this paper is to present data from two source-receiver geometries that display anomalously late SP_dKS times relative to SKS. The main conclusion is that models having relatively low V_P values at the base of the mantle can produce synthetics that agree with the mean of the observations.

Data

Long-period (LP) observations (5-15s) from deep focus Tonga events recorded by North American World Wide Seismographic Stations Network (WWSSN) and Canadian Seismographic Network (CSN) stations, and South American events recorded by European and Eurasian WWSSN stations are ideal to study SP_dKS because of the good station coverage spanned over an appropriate distance range. These records have been digitized and rotated to obtain the SV component of motion. Table 1 lists events used in the analysis and Figure 2 displays the corresponding path coverage. Plotted are great-circle paths between events (stars) and stations (triangles). Thicker line segments represent the P diffraction zones associated with SP_dKS waves.

Digitized SV observations for one of the Tonga events and 2 Bolivia events are presented in Figure 3. In both columns, amplitudes are normalized to the SKS peak, and all traces have been aligned to the SKS peak (dotted line). Arrows indicate the peak of the SP_dKS arrival. Moveout of SP_dKS behind SKS is easily viewed in the data. Second order features are also present. For example, the records WES (Westin, Massachusetts) and SJG (San Juan, Puerto Rico) in the Tonga column are nearly at the same distance, but differ in azimuth by about 28°, with SP_dKS at WES arriving almost 2 seconds later than that at SJG. Lateral variations in V_P between the two paths can cause such behavior. Records AAM (Ann Arbor, Michigin) of the Tonga event and JER (Jerusalem, Israel) of the 8-23-68 Bolivia event are both near 108.5°, though only the AAM record shows evidence of SP_dKS. In viewing more AAM and JER records for these source regions, this appears to be a stable pattern. This might be attributed to a high Q path for AAM (the SKS peak is higher frequency than that at JER, see Figure 3), resulting in the ability to view the onset of SP_dKS. Complicated SP_dKS arrivals are apparent at stations TAB (Tabris, Iran) and MSH (Meshed, Iran) for the 8-23-68 Bolivia event. SP_dKS for both records appears as a double arrival. Such a feature may be produced by having different D″ V_P structures on the source and receiver sides of the SP_dKS paths. Also noteworthy is a slight

TABLE 1. Event information as reported by ISC.

Date	Lat.	Lon.	Z	mb	Region
01/24/69	21.87S	179.54W	587	5.9	Fiji-Tonga
06/28/70	21.66S	179.42W	587	5.8	Fiji-Tonga
11/03/65	9.04S	71.32W	587	5.9	Peru-Brazil
08/23/68	21.95S	63.64W	513	5.6	S. Bolivia
10/25/73	21.96S	63.65W	517	6.1	S. Bolivia
12/27/67	21.29S	68.20W	91	6.3	Bolivia
07/25/69	25.49S	63.21W	573	5.6	Argentina

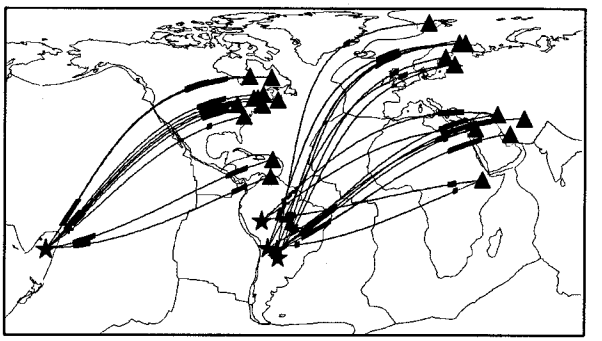

Fig. 2. Great-circle paths between events (stars) and stations (triangles). The thicker line segments represent the P diffraction zones.

negative polarity arrival before SP_dKS at HAL (Halifax, Nova Scotia, Canada) for the Tonga event, and SHI (Shiraz, Iran) and MSH for the 8-23-68 Bolivia event. This arrival is the inner core reflected phase SKiKS.

Synthetic Modeling

As apparent in Figures 1 and 2, the SP_dKS phase depends strongly on CMB mantle-side V_P at both the source and receiver sides of the path. The SP_dKS arrival can appear to be longer period, or even a double arrival, if V_P differs on the two sides of the path. Siver and Bina [1993] discuss such heterogeneity in relation to the SKKS/SKS ratios. These effects have been explored in our experiments using a generalized ray code that permits differing V_P mantle structures for the downgoing and upgoing SP_dKS waves. In this paper, however, we will concentrate on understanding the first order anomalous features in the data, such as the SP_dKS-SKS differential times and

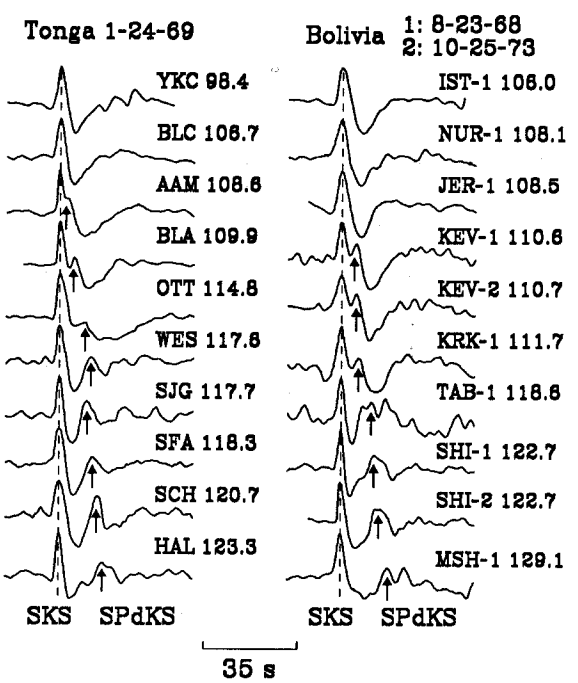

Fig. 3. SV data for a Tonga event recorded in North America (left column) and 2 Boliva events recorded in Europe and Eurasia (right column). SKS is lined up and amplitudes are normalized. Arrows indicate the SP_dKS arrival

waveshapes. Since most of the data analyzed here has clean, single-peak SP_dKS arrivals, we approach the first order modeling in the 1-D sense.

The reflectivity method has been employed to ensure proper handling of all important multiples within the CMB region. SV motions of SKS and SP_dKS have been produced and convolved with a LP WWSSN instrument for comparison to the data. Figure 4 displays such synthetics for the PREM reference model [Dziewonski and Anderson, 1981], and two models containing perturbations of PREM in the bottom 100 km of the mantle. The source depth in the synthetics is 560 km. The development of the first visible SP_dKS arrival in the PREM synthetics occurs at a larger distance than in the data (compare with Figure 3). The shift in distance to match the SP_dKS-SKS times of the data and the PREM synthetics is 2-3°. Also in Figure 4 are synthetics for models containing a 5% decrease in V_P at the CMB from that of PREM, with a linear gradient above connecting to PREM 50 and 100 km above the CMB (models P-5_50 and P-5_100, middle and right panels, respectively.) The SP_dKS travel time curve of PREM is super-imposed on the P-5_50 and P-5_100 synthetics to illustrate the increased SP_dKS-SKS times by decreasing V_P at the base of the mantle. Model P-5_100 produces larger SP_dKS-SKS times due to the thicker zone of reduced V_P. The SP_dKS-SKS times and the first distance that SP_dKS is visible for the P-5_100 model is compatible with the mean of the observations. These models are meant to illustrate the type of V_P reductions necessary to match the SP_dKS-SKS times and waveforms, but are certainly non-unique. There is also the problem of lateral variations, between the source and receiver sides of the path at the CMB, as well as between the South America and Fiji-Tonga data sets. This will be discussed in the next section.

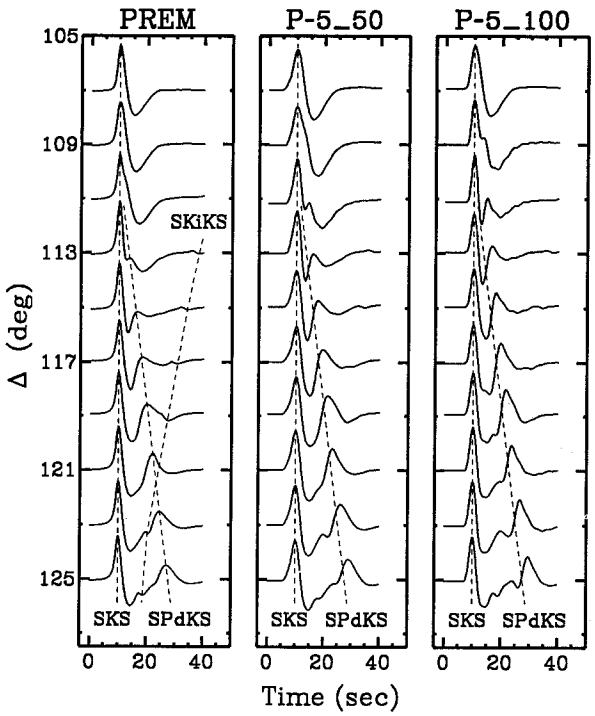

Fig. 4. PREM LP WWSSN synthetics of SKS and SP_dKS (and SKiKS) for models tested in this study.

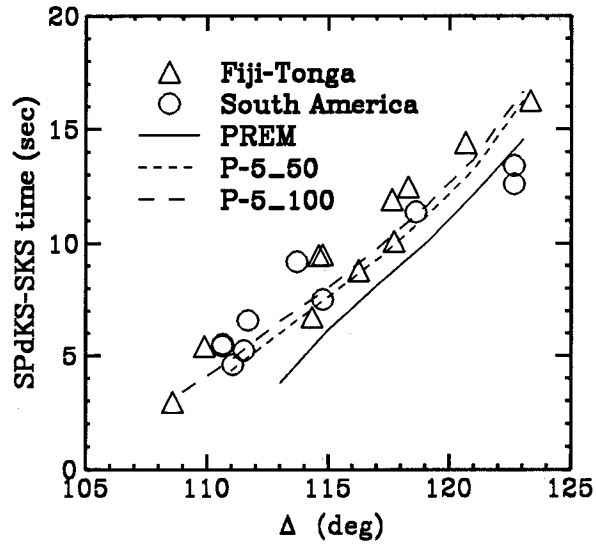

Fig. 5. Peak to peak differential travel times of SP_dKS-SKS for the data (symbols) and the synthetics (lines).

Discussion

As a first effort in understanding the anomalous SP_dKS-SKS times, we have explored 1-D models that contain perturbations to PREM in the lowermost 50-100 km of the mantle. In this approach, there is a trade-off between V_P at the CMB and the thickness of the layer over which the V_P values depart from PREM. However, synthetic tests varying V_P and V_S lower mantle structure, as well as outer core V_P structure, show that SP_dKS-SKS times are most strongly affected by the mantle V_P value at the CMB interface. The other features investigated only produced second order effects on the synthetics. The thickness of the low-velocity zone (LVZ) at the base of the mantle necessary to model the data depends on the wavelengths of interest. For the LP WWSSN data, an LVZ 50 km thick can model the anomalies if V_P is lowered by 6% (to 12.9 km/s). Broadband data will help to resolve this non-uniqueness through investigating frequency dependence of SP_dKS waves.

The differential times (peak to peak) of SP_dKS and SKS are summarized in Figure 5. Also included are those of the models in Figure 4. The SP_dKS-SKS curves deviate from straight lines due to the interference of SP_dKS with the back swing of the SKS phase. The first order feature apparent in Figure 5 is that PREM under-predicts the SP_dKS-SKS times by 2-3 sec on average. Predictions from model P-5_100 fit the average of the data, with scatter in the data on the order of 1-2 sec. The two data points near 123° have anomalously small times (records SHI-1,2, Figure 3). This implies that the source and receiver side P diffraction zones for paths to SHI from South America average to a more PREM-like V_P at the CMB (or faster.) All the other data in the figure, however, require anomalously slow V_P values at the CMB, with large lateral variations in V_P (and probably dV_P/dz) necessary to explain the scatter.

Anisotropic media can cause distortions and splitting in broadband SKS waveforms [see, e.g., Silver and Chan, 1988]. Such effects, however, are not observed for the LP WWSSN and CSN data, and hence are assumed not to contribute to the scatter seen in Figure 5. Also, synthetic tests

show that SP_dKS-SKS times and waveforms are insensitive to small perturbations (± 5 km) in CMB depth, or event source depth. The first order analysis of this paper does not address discontinuity structures at the top of the D″ layer (which only produce second order effects on SP_dKS). A ±50 km event mislocation along azimuth will contribute ±0.4 sec to the SP_dKS-SKS times. If small scale-length lateral variations in V_S exist at the base of the mantle, then SKS or SP_dKS may be preferentially affected. For 5-15 sec waves traveling at 7.2 km/s, wavelengths are 36-108 km, which is smaller than the separation between SKS and SP_dKS for a large part of the distance range in Figure 1b (dotted line). A 1% reduction in V_S over a 200 km layer at the base of the mantle traversed only by SP_dKS (and not SKS) will increase the SP_dKS-SKS time by 0.6 sec, if the same anomaly exists at the core entrance and exit locations. A similar scenario with a 2% reduction in V_S will result in a 1.2 sec increase of the difference time. We are unable to resolve such features, however, since the data are scattered at distances where SKS and SP_dKS paths are separated by less than a wavelength in D″ (109-112°, see Figure 5). Other factors, such as laterally varying CMB V_P must be contributing to the scatter.

If the anomalously low CMB V_P values needed to model the SP_dKS data are linearly connected to the overlying mantle of the PREM model (as done for models P-5_50 and P-5_100), super-critical velocity gradients and thus departures from adiabaticity result. Better resolving the vertical V_P structure at the base of the mantle is necessary, and can provide important information about the thermal boundary layer at the base of the mantle. Analyzing more data, along with the inclusion of broadband data, will help in this matter.

Past seismological studies of the radial velocity structure in the D″ region have resulted in velocity gradients ranging from very negative to slightly positive [see Young and Lay, 1987, for a review]. Reconciling the strongly negative gradient implied from this study with contrasting positive (or slightly negative) gradients of past studies remains a task for future work. Silver and Bina [1993] point out the affect of the sudden drop in SKS amplitudes on SKKS/SKS ratios (at the ScP critical ray parameter) is strongly dependent on mantle-side CMB V_P. For a path geometry similar to ours in the Pacific, they conclude a 2.0-2.5% reduction in CMB V_P is consistent with their observations. SP_dKS data require a larger reduction in V_P, though the agreement in trend for the similar data is encouraging.

Conclusion

Anomalous differential times between LP SP_dKS and SKS are presented for two different source-receiver geometries. The SP_dKS-SKS times most strongly depend on V_P at the base of the mantle near the SKS core entrance and exit locations. The anomalous times can be fit, on average, by models containing a 5% reduction in V_P from PREM at the CMB, distributed over 100 km. This V_P structure above the CMB is non-unique, though the inclusion of more data (along with broadband data) will help better resolve the structure. The scatter in the data suggest lateral variations of the low V_P values.

Acknowledgements. We thank D. L. Anderson and J. Schweitzer for reviews, Xiaoming Ding for the South American data, Harley Benz for help with the synthetics, and an anonymous reviewer for helpful comments. This research was supported by NSF grant EAR-91-17781. Contribution #5303, Division of Geological and Planetary Sciences, California Institute of Technology.

References

Choy, G. L., Theoretical seismograms of core phases calculated by frequency-dependent full wave theory, and their interpretation, *Geophys. J. R. astr. Soc., 51,* 275-312, 1977.

Dziewonski, A. M., and D. L. Anderson, Preliminary reference Earth model (PREM), *Phys. Earth Planet. Int., 25,* 297-356, 1981.

Kind, R., and G. Müller, Computations of *SV* waves in realistic Earth models, *J. Geophys., 41,* 149-172, 1975.

Schweitzer, J., Laufzeiten und Amplituden der Phasen SKS und SKKS und die Struktur des äusseren Erdkerns, Diploma thesis (in German), 117 pp., University of Frankfurt, 1984.

Schweitzer, J., and G. Müller, Anomalous difference traveltimes and amplitude ratios of SKS and SKKS from Tonga-Fiji events, *Geophys. Res. Lett., 13,* 1529-1532, 1986.

Silver, P., and W. W. Chan, Implications for continental structure and evolution from seismic anisotropy, *Nature, 355,* 34-39, 1988.

Silver, P., and C. R. Bina, An anomaly in the amplitude ratio of SKKS/SKS in the range 100-108° from portable teleseismic data, *Geophys. Res. Lett., 20,* 1135-1138, 1993.

Young, C. J., and T. Lay, The core-mantle boundary, *Ann. Rev. Earth Planet. Sci, 15,* 25-46, 1987.

E. J. Garnero and D. V. Helmberger, Seismological Laboratory 252-21, California Institute of Technology, Pasadena, CA, 91125, USA

S. P. Grand, Department of Geological Sciences, University of Texas, P.O. Box 7909, Austin, TX 78715, USA

(Received May 11, 1993
accepted July 8, 1993.)